

New 5-Aminolevulinic Acid Esters—Efficient Protoporphyrin Precursors for Photodetection and Photodynamic Therapy

Author(s): H. Brunner, F. Hausmann, R. Knuechel

Source: Photochemistry and Photobiology, 78(5):481-486.

Published By: American Society for Photobiology

DOI: [http://dx.doi.org/10.1562/0031-8655\(2003\)078<0481:NAAEPP>2.0.CO;2](http://dx.doi.org/10.1562/0031-8655(2003)078<0481:NAAEPP>2.0.CO;2)

URL: <http://www.bioone.org/doi/full/10.1562/0031-8655%282003%29078%3C0481%3ANAAEPP%3E2.0.CO%3B2>

BioOne (www.bioone.org) is a nonprofit, online aggregation of core research in the biological, ecological, and environmental sciences. BioOne provides a sustainable online platform for over 170 journals and books published by nonprofit societies, associations, museums, institutions, and presses.

Your use of this PDF, the BioOne Web site, and all posted and associated content indicates your acceptance of BioOne's Terms of Use, available at www.bioone.org/page/terms_of_use.

Usage of BioOne content is strictly limited to personal, educational, and non-commercial use. Commercial inquiries or rights and permissions requests should be directed to the individual publisher as copyright holder.

New 5-Aminolevulinic Acid Esters—Efficient Protoporphyrin Precursors for Photodetection and Photodynamic Therapy[¶]

H. Brunner^{*1}, F. Hausmann¹ and R. Knuechel²

¹Institute of Inorganic Chemistry, University of Regensburg, Regensburg, Germany and

²Institute of Pathology, University of Regensburg, Regensburg, Germany

Received 14 May 2003; accepted 10 August 2003

ABSTRACT

Photodetection (PD) and photodynamic therapy (PDT) with 5-aminolevulinic acid (ALA)-induced protoporphyrin IX (PPIX) accumulation are approaches to detect and treat dysplasia and early cancer in the gastrointestinal tract and in the urinary bladder. Because ALA-induced PPIX production is limited, we synthesized ALA ester hydrochlorides 3–22 and tested them in two different *in vitro* models (gastrointestinal tract: HT29–CCD18; urinary bladder: J82–URO TSA). PPIX accumulation after incubation with 0.12 mmol/L for 3 h and PPIX accumulation as a function of different incubation times were measured using flow cytometry. 3-(4,5-Dimethylthiazol-2-yl)-2,5-diphenyltetrazolium bromide assays were performed to check cellular dark toxicity. Phototoxicity after irradiation was tested. ALA nonafluorohexylester hydrochloride 11, ALA thiohexylester hydrochloride 13 and ALA dibenzyl diester dihydrochloride 19 induced appreciably increased PPIX levels and showed improved phototoxicity compared with the references ALA hydrochloride 1, ALA hexylester hydrochloride 3 and ALA benzylester hydrochloride 4. Thus, the new compounds 11, 13 and 19 are promising compounds for PD and PDT.

INTRODUCTION

Photodetection (PD) and photodynamic therapy (PDT) are techniques currently under clinical assessment for observation and local destruction of malignant tumors and premalignant lesions. After application of 5-aminolevulinic acid (ALA), an increased metabolic formation of protoporphyrin IX (PPIX) is induced rather specifically in neoplastic tissue. During blue-light excitation, PPIX with its distinct red fluorescence can be used for photodetection or applying higher light doses for PDT (1). In contrast to other photosensitizers such as hematoporphyrin

derivative, PPIX, applied systemically, topically or synthesized from ALA, shows a very short half-life in the body, and photosensitizing effects do not last much longer than 24 h (2). However, ALA-induced PPIX accumulation is limited by the high hydrophilicity of ALA, and therefore fairly high doses are needed to reach clinically relevant concentrations of PPIX. Hydrophilic compounds such as ALA poorly cross biological barriers like cellular membranes (3,4). To overcome this problem, ALA esters have been used as prodrugs instead of ALA itself. Within the cells the ALA esters are hydrolyzed by unspecific esterases to give the parent compound ALA. The improvement of bioavailability of ALA by application of ALA esters is determined by two processes: the rate of diffusion of the prodrug through the cell membrane and its rate of enzymatic conversion into ALA (5). Esterified derivatives of ALA are currently being investigated as a favorable alternative to ALA to increase cellular PPIX contents. In addition to dermatology, possible fields of application of ALA ester-induced PPIX production for PD and PDT are neurosurgery, pneumology, gastroenterology, gynecology, urology and oral surgery.

ALA hydrochloride 1 is increasingly replaced by its esterified derivatives because of their higher PPIX accumulation. In dermatology, ALA methylester hydrochloride 2 is used for PDT of basal cell carcinoma and actinic ceratosis (6). ALA hexylester hydrochloride 3 and ALA benzylester hydrochloride 4 are in clinical trials for PD and PDT of the gastrointestinal tract and the urinary bladder (Fig. 1).

To enhance PPIX accumulation beyond the level achievable with ALA hexylester hydrochloride 3 and ALA benzylester hydrochloride 4, we synthesized the ALA oxalkylester hydrochlorides 5–8, the fluorinated ALA alkylester hydrochlorides 9–12, the ALA thiohexylester hydrochloride 13, the ALA benzylester hydrochlorides 14–19 and miscellaneous other ALA ester hydrochlorides 20–22. PPIX accumulation and phototoxicity were evaluated by *in vitro* studies (7) (Fig. 2).

MATERIALS AND METHODS

The synthesis of compounds 2–6 has been described by Takeya (8) and Berg *et al.* (9).

Thionyl chloride method (8). An excess of the dry commercially available alcohol (20 mL) was cooled to 0°C, and freshly distilled thionyl chloride (3.0 mL, 41.4 mmol) was added. ALA hydrochloride (0.5 g, 3 mmol) was added to the solution. The solution was stirred at 60°C for 5 h. Then, the excess of alcohol was evaporated *in vacuo*. After recrystallization from methanol–diethylether at –20°C, the pure ALA esters 3, 4, 5–8 and 15 were obtained as the hydrochloride salts (Fig. 3).

[¶]Posted on the website on 2 September 2003

*To whom correspondence should be addressed at: Institute of Inorganic Chemistry, University of Regensburg, D-93040 Regensburg, Germany.

Fax: 49-941-943-4439; e-mail: henri.brunner@chemie.uni-regensburg.de

Abbreviations: ALA, 5-aminolevulinic acid; BOC, t-butyloxycarbonyl; DMSO, dimethyl sulfoxide; FCS, fetal calf serum; LD₅₀, lethal dose (50%); MS, mass spectrometry; MTT, 3-(4,5-dimethylthiazol-2-yl)-2,5-diphenyltetrazolium bromide; NMR, nuclear magnetic resonance; PBS, phosphate-buffered saline; PD, photodetection; PDT, photodynamic therapy; PPIX, protoporphyrin IX.

© 2003 American Society for Photobiology 0031-8655/03 \$5.00+0.00

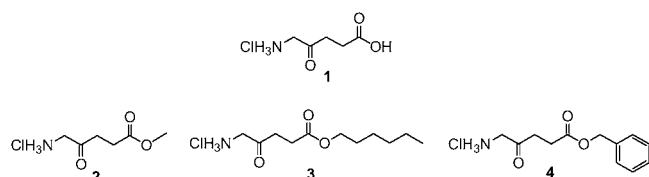


Figure 1. ALA hydrochloride **1**, ALA methylester hydrochloride **2**, ALA hexylester hydrochloride **3** and ALA benzylester hydrochloride **4**.

Carbodiimide coupling. ALA ester hydrochlorides **9–14** and **16–22** were prepared in a three-step synthesis consisting of *t*-butyloxycarbonyl (BOC) protection of ALA hydrochloride (**9**), esterification (**10**) and deprotection. An aqueous solution of ALA hydrochloride (420 mg, 2.5 mmol) in 5 mL of water was adjusted to pH 8.5 with 1 N NaOH. After addition of di-*tert*-butyldicarbonate (1.16 g, 3 mmol) in 5 mL of dioxan, the solution was stirred for 18 h at room temperature. Excess di-*tert*-butyldicarbonate was removed by extraction with diethylether. After acidifying the aqueous solution with 1 N HCl and extraction with ethyl acetate, 5-*tert*-butyloxycarbonyl aminolevulinic acid was obtained as a colorless oil.

To an ice-cooled solution of 300 mg (1.3 mmol) of 5-*tert*-butyloxycarbonyl aminolevulinic acid, 120 mg (1 mmol) of dimethylaminopyridine, 1.5 mmol of the corresponding commercially available alcohol and 257 mg (1.6 mmol) of 1-ethyl-3-[3-dimethyl(aminopropyl)]carbodiimide hydrochloride were added. The solution was stirred for 2 h at 0°C and then for 48 h at room temperature. After evaporation of the solvent, the residue was dissolved in water. Extraction with ethyl acetate, washing the organic layer with 10% aqueous NaHCO₃ solution and removal of the solvent gave the BOC-protected ALA esters, which were purified by column chromatography (SiO₂, MeOH–CH₂Cl₂ 40:1).

To an ice-cooled solution of 0.25 mmol BOC-protected ALA ester in 5 mL of ethyl acetate, 5 mL of HCl-saturated ethyl acetate was added. After 30 min, the ice bath was removed, and the solution was stirred for 3 h at room temperature. Removal of the solvent and recrystallization (ethyl

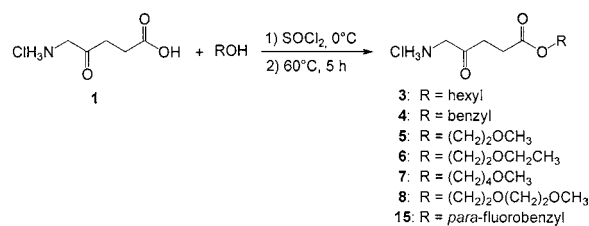


Figure 3. Synthesis of ALA ester hydrochlorides with thionyl chloride.

acetate–petroleum ether) afforded the pure water-soluble ALA ester hydrochlorides (Fig. 4).

¹H-nuclear magnetic resonance and mass spectrometry data. Compound **7:** ¹H-NMR (DMSO-D₆): δ 1.56 (m, 4H, 2CH₂), 2.55/2.80 (AA'BB' system, 4H, 2CH₂), 3.22 (s, 3H, CH₃), 3.32 (m, 2H, CH₂), 3.95 (s, 2H, CH₂), 4.02 (m, 2H, CH₂), 8.31 (s, 3H, NH₃). Mass spectrometry (MS) PI-DCl (NH₃) C₁₀H₂₀ClNO₄ (253.7) m/z (%): 218.1 (MH-HCl, 100). Compound **8:** ¹H-NMR (DMSO-D₆): δ 2.57/2.79 (AA'BB' system, 4H, 2CH₂), 3.30–3.60 (m, 7H, 2CH₂, CH₃), 3.77 (m, 2H, CH₂), 3.97 (s, 2H, CH₂), 4.11 (m, 2H, CH₂), 8.05 (3H, NH₃). MS PI-DCl (NH₃) C₁₀H₂₀ClNO₅ (269.7) m/z (%): 234.0 (MH-HCl, 100). Compound **9:** ¹H-NMR (D₂O): δ 2.73/2.85 (AA'BB' system, 4H, 2CH₂), 4.10 (s, 2H, CH₂), 4.57–4.68 (m, 2H, CH₂). MS PI-DCl (NH₃) C₁₀H₁₂ClF₈NO₃ (349.6) m/z (%): 314.2 (MH-HCl, 100). Compound **10:** ¹H-NMR (D₂O): δ 2.85/2.90 (AA'BB' system, 4H, 2CH₂), 4.10 (s, 2H, CH₂), 4.57–4.68 (t, ³J(H-F) = 13.7 Hz, 2H, CH₂), 6.13–6.67 (tt, ²J(H-F) = 51.1 Hz, ³J(H-F) = 5.5 Hz, 1H, CH). MS PI-DCl (NH₃) C₁₀H₁₂ClF₈NO₃ (381.7) m/z (%): 346.3 (MH-HCl, 100). Compound **11:** ¹H-NMR (D₂O): δ 2.40–2.57 (tt, ³J(H-H) = 6.1 Hz, ³J(H-F) = 19.4 Hz, 2H, CH₂), 2.62/2.79 (AA'BB' system, 4H, 2CH₂), 4.00 (s, 2H, CH₂), 4.34 (t, ³J(H-H) = 6.1 Hz, 2H, CH₂). MS PI-DCl (NH₃) C₁₁H₁₃ClF₉NO₃ (413.7) m/z (%): 378.3 (MH-HCl, 100). Compound **12:** ¹H-NMR (D₂O): δ 2.71/2.84 (AA'BB' system, 4H, 2CH₂), 4.00 (s, 2H, CH₂), 4.76 (m, 2H, CH₂). MS PI-DCl (NH₃) C₁₂H₁₁ClF₁₉NO₃ (499.3) m/z (%): 464.2 (MH-HCl,

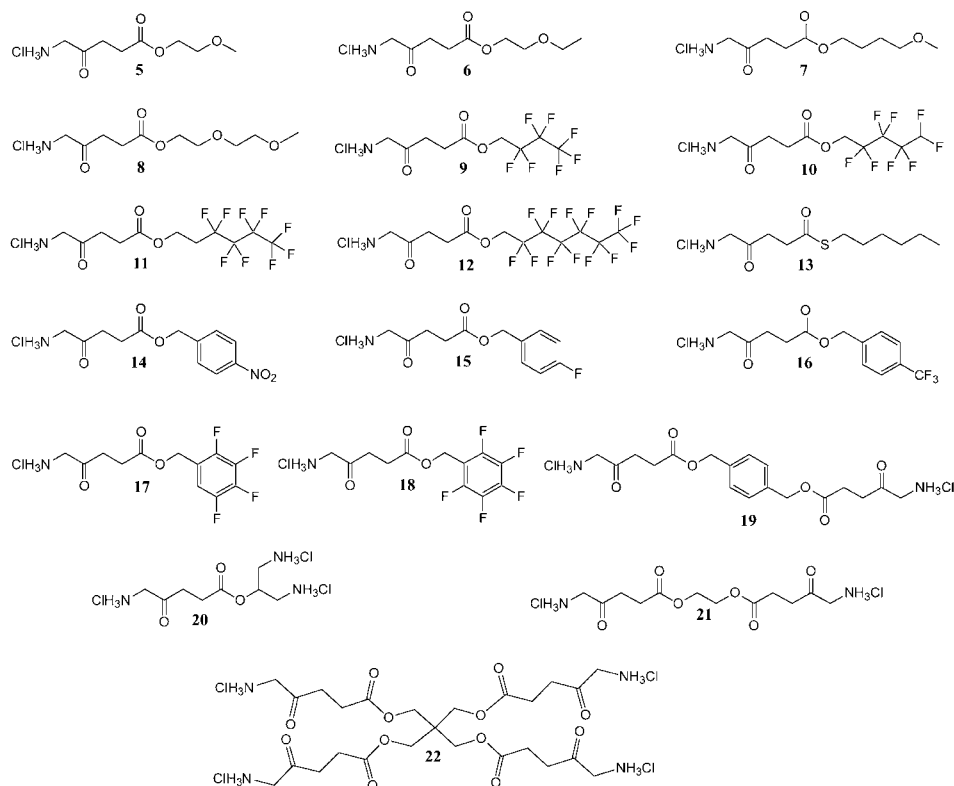


Figure 2. ALA ester hydrochlorides **5–22**.

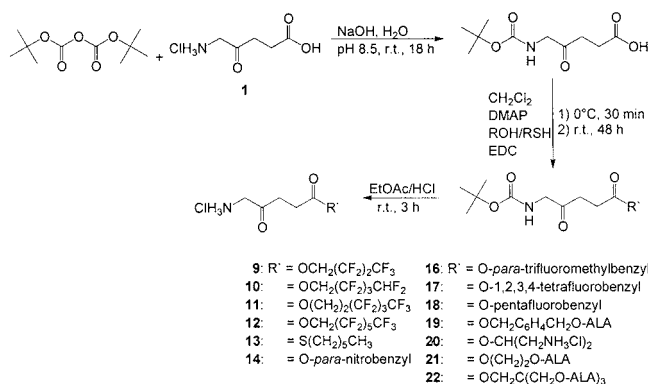


Figure 4. Synthesis of ALA ester hydrochlorides using carbodiimide coupling.

100). Compound **13**: ¹H-NMR (D₂O): δ 0.88 (t, ³J(H-H) = 6.8 Hz, 3H, CH₃), 1.20–1.40 (m, 6H, 3CH₂), 1.55 (m, 2H, CH₂), 2.79–3.14 (m, 6H, 3CH₂), 4.27 (s, 2H, CH₂), 8.17 (br. s, 3H, NH₃). MS PI-DCI (NH₃) C₁₁H₂₂ClNO₅S (267.8) m/z (%): 232.2 (MH-HCl, 100). Compound **14**: ¹H-NMR (D₂O): δ 2.70/2.82 (AA'BB' system, 4H, 2CH₂), 3.99 (s, 2H, CH₂), 5.16 (s, 2H, CH₂), 7.48/8.13 (AA'BB' system, 4H, 4CH). MS PI-DCI (NH₃) C₁₂H₁₅ClN₂O₅ (302.7) m/z (%): 267.3 (MH-HCl, 100). Compound **15**: ¹H-NMR (D₂O): δ 2.62/2.83 (AA'BB' system, 4H, 2CH₂), 3.98 (s, 2H, CH₂), 5.08 (s, 2H, CH₂), 7.19/7.41 (AA'BB' system, 4H, 4CH). MS PI-DCI (NH₃) C₁₂H₁₅ClFNO₃ (275.7) m/z (%): 240.3 (MH-HCl, 66), 133.1 (100). Compound **16**: ¹H-NMR (D₂O): δ 2.65/2.80 (AA'BB' system, 4H, 2CH₂), 4.08 (s, 2H, CH₂), 5.10 (s, 2H, CH₂), 7.45/7.62 (AA'BB' system, 4H, 4CH). MS PI-DCI (NH₃) C₁₃H₁₅ClF₃NO₃ (325.7) m/z (%): 290.4 (MH-HCl, 100). Compound **17**: ¹H-NMR (D₂O): δ 2.65/2.80 (AA'BB' system, 4H, 2CH₂), 4.08 (s, 2H, CH₂), 5.10 (s, 2H, CH₂), 7.12 (m, 1H, CH). MS ESI (CH₃OH, 1% HAc) C₁₂H₁₂ClF₄NO₃ (329.7) m/z (%): 294.0 (MH-HCl, 100). Compound **18**: ¹H-NMR (D₂O): δ 2.59/2.79 (AA'BB' system, 4H, 2CH₂), 3.98 (s, 2H, CH₂), 5.17 (s, 2H, CH₂). MS PI-DCI (NH₃) C₁₂H₁₁ClF₅NO₃ (347.7) m/z (%): 312.1 (MH-HCl, 62.2); 133.1 (100). Compound **19**: ¹H-NMR (D₂O): δ 2.64/2.81 (AA'BB' system, 8H, 4CH₂), 3.98 (s, 4H, 2CH₂), 5.05 (s, 4H, 2CH₂), 7.32 (s, 4H, 4CH). MS ESI (CH₃OH, 1% HAc) C₁₈H₂₆Cl₂N₂O₆ (437.3) m/z (%): 365.0 (MH-2HCl, 100). Compound **20**: ¹H-NMR (D₂O): δ 2.72/2.87 (AA'BB' system, 4H, 2CH₂), 3.22–3.28 (m, 4H, 2CH₂), 3.98 (m, 1H, CH), 4.02 (s, 2H, CH₂). MS ESI (CH₃OH, 1% HAc) C₈H₂₀Cl₃N₃O₃ (312.6) m/z (%): 203.8 (MH-3HCl, 100). Compound **21**: ¹H-NMR (D₂O): δ 2.62/2.81 (AA'BB' system, 8H, 4CH₂), 4.15 (s, 4H, 2CH₂), 4.23 (s, 4H, 2CH₂). MS ESI (CH₃OH, 1% HAc) C₁₂H₂₂Cl₂N₂O₆ (361.2) m/z (%): 288.9 (MH-2HCl, 100). Compound **22**: ¹H-NMR (D₂O): δ 2.65/2.83 (AA'BB' system, 16H, 8CH₂), 3.97–4.15 (m, 16H, 8CH₂). MS ESI (CH₃OH/H₂O, 1% HAc) C₂₅H₄₄Cl₄N₄O₁₂ (734.5) m/z (%): 589.2 (MH-4HCl, 15); 295.2 (1/2(M-4HCl) + H, 100).

Cell lines. The human adenocarcinoma cell line HT29 and the human colonic fibroblast cell line CCD18 were used as an *in vitro* model for the gastrointestinal tract. For the urothelium the human urothelial carcinoma cell line J82 and the human urothelial cell line UROTSA were chosen as an *in vitro* model. The cell line HT29 [G2] was maintained in Dulbecco modified Eagle medium (Sigma, Deisenhofen, Germany) supplemented with 5% fetal calf serum (FCS; Sigma). The cell line CCD18 was maintained in modified Eagle medium + 10% FCS. The urothelial cell lines J82 [G3] and UROTSA were maintained in Roswell Park Memorial Institute 1640 medium (Biochrom, Berlin, Germany) supplemented with 5% FCS, 1% L-glutamine and 1% sodium pyruvate (GIBCO, Eggenstein, Germany) and were kept at 37°C in a humidified atmosphere containing 5% carbon dioxide. Cells were subcultured before reaching plateau growth using 0.1% trypsin–0.04% ethylenediaminetetraacetic acid (GIBCO) in phosphate-buffered saline (PBS; Biochrom). Experiments were performed with postconfluent cells (cell density/growth period: HT29, 5 × 10⁴/cm²/7 days; CCD18, 1 × 10⁴/cm²/8 days; J82, 6 × 10³/cm²/8 days; UROTSA, 6 × 10³/cm²/10 days).

Incubation. Stock solutions of ALA hydrochloride **1** and ALA ester hydrochlorides **3–22** were prepared in deionized water at a concentration of 0.6 mol/L and stored at –20°C. For each experiment, the stock solution was diluted with culture medium without FCS. Before addition of ALA–ALA ester solutions, the cell layer was rinsed with PBS to remove remaining

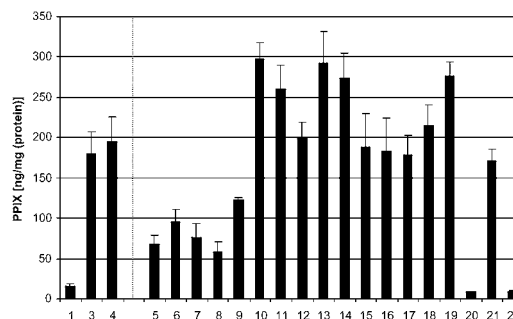


Figure 5. PPIX accumulation measured by flow cytometry in colon carcinoma cell line HT29 induced by the references ALA hydrochloride **1**, ALA hexylester hydrochloride **3**, ALA benzylester hydrochloride **4** and ALA ester hydrochlorides **5–22** (0.12 mmol/L, 3 h).

FCS. Cells were cultivated in six well plates and incubated with ALA and ALA esters for 5–180 min at 37°C in the dark using an incubation volume of 2 mL. In subsequent handling, care was taken to avoid exposure to light.

Determination of ALA-induced fluorescence by flow cytometry. After incubation, cells were trypsinized, removed from the six well plates and resuspended in medium without FCS to yield a cell concentration of about 5 × 10⁵ cells/mL. The cellular fluorescence was quantified by a FACScalibur cytometer (Becton-Dickinson, Heidelberg, Germany). ALA-induced fluorescence was excited by an argon ion laser emitting at 488 nm and collected by a photomultiplier after passing through a 670 nm long-pass filter. The flow rate was adjusted to about 2000 events/s, and 2 × 10⁴ events were recorded for each sample. The same instrument settings were used for all experiments. The stability of the cytometer was maintained by weekly calibration using the AUTOCOMP software (Becton-Dickinson). Data were recorded and analyzed with the CellQuest program (Becton-Dickinson). Debris and cell aggregates were excluded from analysis using forward and side scatter signals. To compensate for autofluorescence, the mean fluorescence of ALA–ALA ester-incubated cells was determined by correcting with the mean fluorescence of sham-treated control cells in each individual experiment. To relate fluorescence intensities with PPIX concentrations, PPIX levels (ng/mg protein) were calculated by correlating from a calibration curve obtained by an extraction method as described by Krieg *et al.* (11)

Screening of compounds. To identify promising ALA derivatives for PD and PDT, a screening of ALA hydrochloride **1** and ALA ester hydrochlorides **3–22** was performed. The four human cell lines (HT29–CCD18, J82–UROTSA) were incubated for 3 h with ALA hydrochloride **1** and ALA ester hydrochlorides **3–22** using a concentration of 0.12 mmol/L. PPIX accumulation was quantified using flow cytometry. 3-(4,5-Dimethylthiazol-2-yl)-2,5-diphenyltetrazolium bromide (MTT) assays were carried out as described by Hausmann (7) to ensure that ALA and ALA esters did not show cellular toxicity.

Time-dependent measurements. To optimize the use of ALA esters in PD and PDT, the carcinoma cell lines HT29 and J82 were incubated with ALA hydrochloride **1** and ALA ester hydrochlorides **3, 4, 11, 13** and **19** using different incubation times (5, 30, 180 min, 0.12 mmol/L). After the respective incubation periods, the cells were washed with PBS, and new culture medium without ALA or ALA esters was added. After altogether 3 h of metabolization, PPIX accumulation was measured using flow cytometry.

Phototoxicity measurements. For quantification of PPIX-induced phototoxicity, the cell lines HT29 and CCD18 were incubated (0.12 mmol/L, 3 h) with ALA hydrochloride **1** and ALA ester hydrochlorides **3, 11, 13** and **19** in medium without FCS. After incubation, the cells were irradiated using an incoherent xenon light source (λ = 590–700 nm). Energy densities of 0–30 J/cm² were applied. Irradiated cells were cultivated for 24 h. Then, they were trypsinized and seeded in 96 well plates. After 24 h of growth, MTT tests were performed to examine cellular vitality.

Data analysis and statistics. All experiments were performed at least three times. Data are presented as mean and standard deviation of the mean. Fluorescence kinetics were fitted according to the Michaelis Menten model using Sigma Plot 2.0 (Jandel Corporation, San Raphael, CA). For quantification of phototoxicity, the cellular vitalities in dependence on applied energy densities were fitted according to a four-parametric function

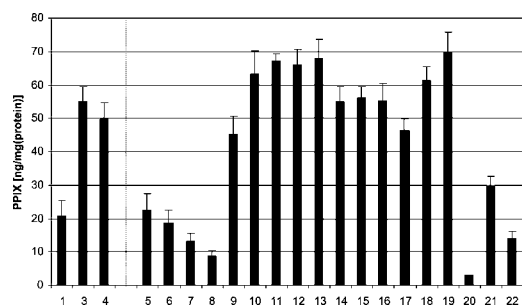


Figure 6. PPIX accumulation measured by flow cytometry in urothelial carcinoma cell line J82 induced by the references ALA hydrochloride **1**, ALA hexylester hydrochloride **3**, ALA benzylester hydrochloride **4** and ALA ester hydrochlorides **5–22** (0.12 mmol/L, 3 h).

using Sigma Plot 2.0. Using these data, values of lethal dose (50%) (LD₅₀) were determined.

RESULTS

In a flow cytometric screening, the PPIX accumulation efficiency of ALA hydrochloride **1** and ALA ester hydrochlorides **3–22** was examined. The resulting PPIX levels in HT29 after incubation with 0.12 mmol/L for 3 h are presented in Fig. 5. PPIX accumulation ranged from 9.3 to 292.1 ng PPIX/mg protein. ALA hydrochloride **1** induced a very low PPIX level, whereas the commercial ALA hexylester hydrochloride **3** and ALA benzylester hydrochloride **4** established PPIX levels of the order of 180–195 ng PPIX/mg protein, which successful new ALA esters have to exceed. ALA oxalkylester hydrochlorides **5–8** and ALA ester hydrochlorides **20–22** were not able to generate significant PPIX levels except **21**, which matched the levels generated by **3** and **4**.

In the series of the fluorinated ALA alkylester hydrochlorides **9–13**, the short-chain C₄ derivative did not achieve the level of **3** and **4**, whereas the long-chain C₇ derivative did. Interestingly, the middle-chain C₅ and C₆ derivatives **10** and **11** definitely outperformed references **3** and **4** in the PPIX accumulation (Fig. 5). The same was true for ALA thiohexylester hydrochloride **13**.

In the group of the ALA benzylester hydrochlorides **14–19** the fluorinated ALA benzylester hydrochlorides **15–18** generated similar PPIX contents as **3** and **4**. Interestingly, ALA nitrobenzylester hydrochloride **14** and ALA dibenzylester dihydrochloride **19** surpassed **3** and **4** appreciably (Fig. 5).

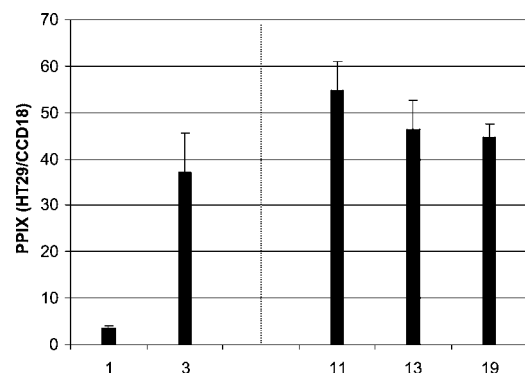


Figure 7. PPIX ratios (HT29–CCD18) induced by the references ALA hydrochloride **1**, ALA hexylester hydrochloride **3** and ALA ester hydrochlorides **11**, **13** and **19** (0.12 mmol/L, 3 h).

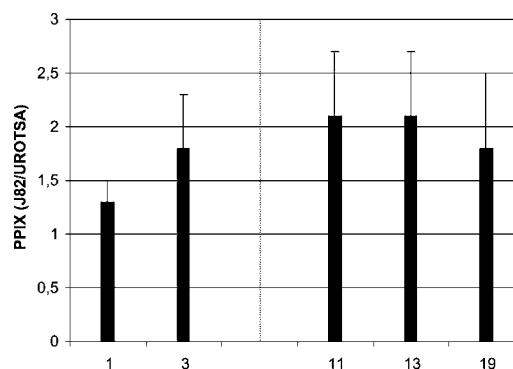


Figure 8. PPIX ratios (J82–UROTSA) induced by the references ALA hydrochloride **1**, ALA hexylester hydrochloride **3** and ALA ester hydrochlorides **11**, **13** and **19** (0.12 mmol/L, 3 h).

Compared with HT29 the colon fibroblast cell line CCD18 led to very low PPIX accumulation levels, ranging from 3.9 to 6.3 ng PPIX/mg protein (7) (data not shown). For the most successful compounds **11**, **13** and **19** the PPIX accumulation in CCD18 cells can be calculated from the HT29–CCD18 ratios given together with those of the reference compounds **1** and **3** in Fig. 7 (see below).

PPIX levels induced in J82 cells by ALA hydrochloride **1** and ALA ester hydrochlorides **3–22** ranged from 14.2 to 69.8 ng PPIX/mg protein as shown in Fig. 6. It is obvious that the overall trend is very similar to the results for the HT29 cells shown in Fig. 5. Importantly, the fluorinated ALA ester hydrochlorides **10–12**, ALA thiohexylester hydrochloride **13** and ALA benzylester dihydrochloride **19** exceeded the reference compounds **3** and **4**. Thus, compared with the HT29 cells in the experiments with J82 cells the fluorinated compound **12** improved and the benzylester **14** fell back, leaving **11**, **13** and **19** as the most promising compounds successful in both systems.

PPIX ratios between tumor cells and normal cells were formed for the pairs HT29–CCD18 (gastrointestinal tract model) and J82–UROTSA (urinary bladder model). Enrichment factors for **11**, **13** and **19** are 45–55 for HT29–CCD18 (Fig. 7) and 1.7–2.2 for J82–UROTSA (Fig. 8) in both systems, being higher than for the reference compounds **1** and **3**.

MTT assays were performed to ensure that the new ALA ester hydrochlorides did not show dark toxicity. No significant cellular dark toxicity was obtained for any MTT-tested compound (data not shown), when compared with sham-treated controls (7).

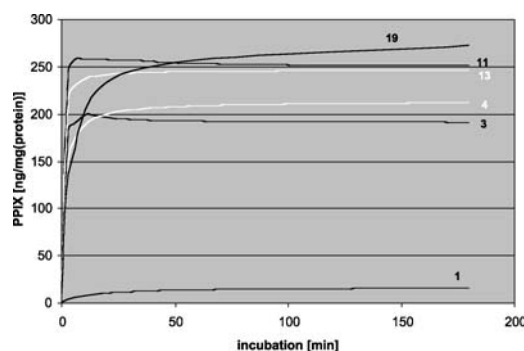


Figure 9. Time-dependent PPIX accumulation in HT29 induced by the references ALA hydrochloride **1**, ALA hexylester hydrochloride **3**, ALA benzylester hydrochloride **4** and ALA ester hydrochlorides **11**, **13** and **19**. Abscissa: incubation time with ALA derivatives followed by 3 h of metabolism as described in the Materials and Methods.

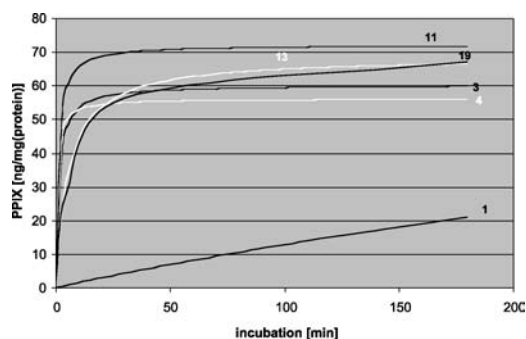


Figure 10. Time-dependent PPIX accumulation in J82 induced by the references ALA hydrochloride **1**, ALA hexylester hydrochloride **3**, ALA benzylester hydrochloride **4** and ALA ester hydrochlorides **11**, **13** and **19**. Abscissa: incubation time with ALA derivatives followed by 3 h of metabolization as described in the Materials and Methods.

The time dependence of PPIX accumulation is shown in Fig. 9 (HT29) and Fig. 10 (J82). In the measurement of the time-dependent PPIX accumulation in HT29 cells (Fig. 9), ALA **1** gave low PPIX levels, whereas ALA hexylester hydrochloride **3** and ALA benzylester hydrochloride **4** induced a steep increase in PPIX formation. Interestingly, the new compounds **11** and **13** showed the same steep increase, achieving PPIX levels clearly above those achieved by **3** and **4**. The curve of **19** grew more slowly. However, after 10 min it exceeded the curves of **3** and **4** and continued to grow after 50 min, producing the highest PPIX levels of all the compounds tested.

In the time-dependence studies of PPIX accumulation in the cell line J82 (Fig. 10), ALA **1** formed more PPIX than in the HT29 cell line, although it still strongly fell behind all the esters that show a behavior similar to that shown in Fig. 9. After about 30 min, the curves of the new esters **13** and **19** exceeded the curves of **3** and **4**. The curve of the fluorinated ALA ester hydrochloride **11** showed the steepest increase in PPIX accumulation and stayed above the curves of all the other tested compounds within the time period of 3 h.

To examine the efficiency of the new compounds for PDT, phototoxicity experiments were performed. In Fig. 11, phototoxicity curves of ALA hydrochloride **1**, ALA hexylester hydrochloride **3** and the new ALA ester hydrochlorides **11**, **13** and **19** are shown for HT29. Cellular vitalities were obtained using MTT assays (7) correlated to nonirradiated controls. The curve of ALA **1** demonstrated that no decrease in the cellular vitality occurred for applied energy densities smaller than 5 J/cm², whereas ALA

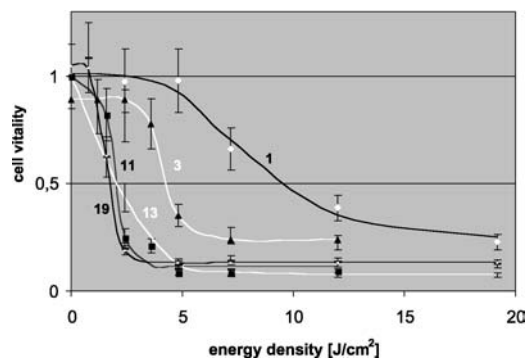


Figure 11. Phototoxicity induced by the references ALA hydrochloride **1**, ALA hexylester hydrochlorides **3** and ALA ester hydrochlorides **11**, **13** and **19** in HT29.

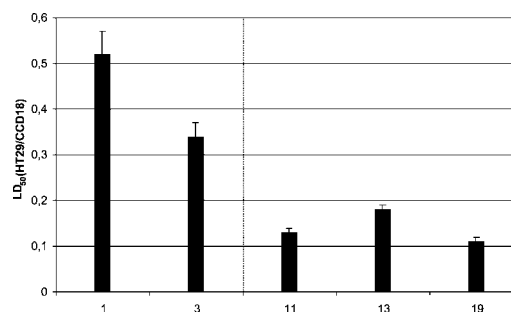


Figure 12. LD₅₀ ratios (HT29–CCD18) induced by the references ALA hydrochloride **1**, ALA hexylester hydrochloride **3** and ALA ester hydrochlorides **11**, **13** and **19**.

hexylester hydrochloride **3** induced a remarkable decrease in cellular vitality already at about 3.5 J/cm². For the new compounds **11**, **13** and **19**, a steep decrease in cellular vitality was observed using energy densities higher than 1 J/cm².

The higher phototoxicity of ALA ester hydrochlorides **11**, **13** and **19** with respect to ALA **1** and ALA hexylester hydrochloride **3** is a consequence of higher PPIX accumulation. Thus, energy densities necessary for reducing cellular vitality (LD₅₀ values) could be minimized by the new compounds **11**, **13** and **19** (LD₅₀: 1.8–2.1 J/cm²) compared with the references ALA **1** (LD₅₀: 9.7 J/cm²) and ALA hexylester hydrochloride **3** (LD₅₀: 4.3 J/cm²).

The ratios of LD₅₀ values between tumor cells and normal cells (HT29–CCD18) were calculated (Fig. 12). Small LD₅₀ ratios mean a predominant destruction of cancerous cells compared with normal tissue under identical conditions. In this regard, LD₅₀ ratios were greatly reduced by ALA ester hydrochlorides **11**, **13** and **19** (0.11–0.18). The references ALA hydrochloride **1** (0.52) and ALA hexylester hydrochloride **3** (0.32) showed much higher ratios.

DISCUSSION

In vitro studies of ALA esters had shown that ALA hexylester hydrochloride **3** and ALA benzylester hydrochloride **4** induced high intracellular PPIX levels (6). Lengthening or shortening as well as branching the alkyl chain of the esters led to a reduction in PPIX accumulation (12). The present study examines the effects of new ALA esters on ALA-induced PPIX accumulation in two *in vitro* models for the gastrointestinal tract and the urinary bladder. Several factors contribute to the success of ALA esters. Fast cellular uptake and rapid ester hydrolysis are prerequisites for high intracellular PPIX levels induced by ALA esters. Both diffusion across cell membranes and enzymatic conversion into ALA are influenced by steric and electronic effects.

Depending on the solubility of ALA hydrochloride **1** in the corresponding alcohol, two different procedures, the thionyl chloride method and the carbodiimide coupling involving BOC protection, esterification and deprotection, were used to synthesize ALA ester hydrochlorides **3–22** in good yields.

Fluorinated ALA alkylesters, especially ALA nonafluorohexylester hydrochloride **11**, induced high PPIX levels. Obviously, the electron-withdrawing effect of the fluoro substituents activated the esters for nucleophilic attack, and ester hydrolysis occurred more rapidly than in nonactivated esters, leading to PPIX contents, which exceeded those achievable with the references ALA hexylester hydrochloride **3** and ALA benzylester hydrochloride **4**. Because ALA amides afforded only low PPIX levels (7), we

investigated ALA thiohexylester hydrochloride **13**, the thio analogue of ALA hexylester hydrochloride **3**, which also should be hydrolysed easily. In fact, ALA thiohexylester hydrochloride **13** gave a distinctly higher PPIX accumulation than ALA hexylester hydrochloride **3**. In this case, a beneficial effect for PPIX accumulation could be the stimulation of ALA dehydrogenase by the hexanethiol formed during hydrolysis (13). In our ester screening, ALA dibenzyl diester dihydrochloride **19**, containing two times the effective benzylester substructure, turned out to be another promising prodrug exceeding the PPIX levels established by the references **3** and **4**.

Summarizing, in a series of experiments, new ALA ester hydrochlorides, in particular **11**, **13** and **19**, proved to be superior to ALA hydrochloride **1** as well as its hexyl and benzyl esters **3** and **4**, respectively. Measurement of PPIX accumulation (0.12 mmol/L for 3 h) and determination of time-dependent PPIX formation showed that ALA ester hydrochlorides **11**, **13** and **19** induced higher PPIX levels compared with compounds **1**, **3** and **4**. Furthermore, PPIX ratios between tumor cells and normal cells were increased for **11**, **13** and **19**. As a consequence of the higher PPIX accumulation, the new ALA ester hydrochlorides **11**, **13** and **19** afforded improved phototoxicity with respect to the reference substances, resulting in lower LD₅₀ values. Thus, the new ALA ester hydrochlorides **11**, **13** and **19** exhibiting no dark toxicity are promising candidates for photodynamic diagnosis and PDT. Further investigations on animal models such as ulcerative colitis will have to demonstrate the suitability of the new esters **11**, **13** and **19** (14). It is well known that *in vitro* properties of ALA esters are quite different from their *in vivo* properties. Therefore, esters poorly performing in this study might show better performance in *in vivo* studies.

Acknowledgement—This study was supported by grant 96.081.2 from the Wilhelm-Sander-Stiftung.

REFERENCES

- Dougherty, T. J., J. E. Kaufman, A. Goldfarb, K. R. Weishaupt, D. G. Boyle and A. Mittleman (1978) Photoradiation therapy for the treatment of malignant tumors. *Cancer Res.* **38**, 2628–2635.
- Kennedy, J. C., R. H. Pottier and D. C. Pross (1990) Photodynamic therapy with endogenous protoporphyrin IX: basic principles and present clinical experience. *Photochem. Photobiol.* **6**, 143–148.
- Eleouet, S., N. Rousset, J. Carre, L. Bourre, V. Vonarx, Y. Lajat, G. M. J. Beijersbergen van Henegouwen and T. Patrice (2000) *In vitro* fluorescence, toxicity and phototoxicity induced by delta-aminolevulinic acid (ALA) or ALA-esters. *Photochem. Photobiol.* **71**, 447–454.
- Kloek, J. and G. M. J. Beijersbergen van Henegouwen (1996) Prodrugs of 5-aminolevulinic acid for photodynamic therapy. *Photochem. Photobiol.* **64**, 994–1000.
- Buundgard, H. (1985) *Design of Prodrugs*. Elsevier, New York.
- Giersckky, K. E., J. Moan, Q. Peng, H. Steen, T. Warloe and A. Bjorseth (1996) Preparation of esters of 5-aminolevulinic acid as photosensitizing agents in photochemotherapy. *PCT Int. Appl.* WO 9628412.
- Hausmann, F. (2003) 5-Aminolävulinsäureester in Tumortherapie und Tumordiagnostik. Ph.D. thesis, University of Regensburg, Regensburg, Germany.
- Takeya, H. (1992) Preparation of 5-aminolevulinic acid alkyl esters as herbicides. Jpn. Kokai Tokkyo Koho, JP4009360. [*Chem. Abstr.* **116**, P189633]
- Berg, Y., A. Greppi, A. O. Siri, R. Neier and L. Juillerat-Jeanerret (2000) Ethylene glycol and amino acid derivatives of 5-aminolevulinic acid as new photosensitizing precursors of protoporphyrin IX in cells. *J. Med. Chem.* **43**, 4738–4746.
- Dhaon, M. K., R. K. Olson and K. Ramasamy (1982) Esterification of N-protected α -amino acids with alcohol/carbodiimide/4-(dimethylamino)-pyridine. Racemization of aspartic and glutamic acid derivatives. *J. Org. Chem.* **47**, 1962–1965.
- Krieg, R. C., S. Fickweiler, O. S. Wolfbeis and R. Knuechel (2000) Cell-type specific protoporphyrin IX metabolism in human bladder cancer *in vitro*. *Photochem. Photobiol.* **72**, 226–233.
- Brunner, H., F. Hausmann, R. C. Krieg, E. Endlicher, J. Schölmerich, R. Knüchel and H. Messmann (2001) The Effects of 5-aminolevulinic acid esters on protoporphyrin IX production in human adenocarcinoma cell lines. *Photochem. Photobiol.* **74**, 721–725.
- Hückel, D. and D. Beyersmann (1979) Rapid purification and direct spectrophotometric assay for 5-aminolevulinic acid dehydratase. *Anal. Biochem.* **97**, 277–281.
- Endlicher, E., P. Rümmele, F. Hausmann, R. Krieg, R. Knüchel, H. C. Rath, J. Schölmerich and H. Messmann (2001) Protoporphyrin IX distribution following local application of 5-aminolevulinic acid and its esterified derivatives in the tissue layers of the normal rat colon. *Br. J. Cancer* **85**, 1572–1576.